Translational Oncology 52 (2025) 102256

Contents lists available at ScienceDirect

Translational Oncology

journal homepage: www.elsevier.com/locate/tranon

Original Research

LPCAT3 regulates the proliferation and metastasis of serous ovarian cancer by modulating arachidonic acid

Fang Wen [a,1], Hongjian Ling [a,1], Rui Ran [a], Xinya Li [a], Houmei Wang [a], Qianfen Liu [b], Min Li [a,*], Tinghe Yu [a,*]

[a] Laboratory of Obstetrics and Gynecology, The Second Affiliated Hospital, Chongqing Medical University, Chongqing, China
[b] Women and Children's Hospital, Chongqing Medical University (Chongqing Health Center for Women and Children), China

ARTICLE INFO

Keywords:
Ovarian cancer
LPCAT3
Lipid metabolism
Arachidonic acid
Ferroptosis

ABSTRACT

Background: Lysophosphatidylcholine acyltransferase 3 (LPCAT3) promotes ferroptosis through the incorporating polyunsaturated fatty acids into membrane phospholipids, however, its role in serous ovarian cancer remains unclear. Here explored cancer proliferation and metastasis after modulating LPCAP3.
Methods: LPCAT3 protein in ovarian cancer tissues was detected using bioinformatic and immunohistoche mical assays. Cell behaviors were observed after up- or down-regulating LPCAT3. Lipid metabolites were determined, and then the pathway enrichment analysis was performed.
Results: The expression level of LPCAT3 in serous ovarian cancer tissues was lower than that in other types of ovarian cancer, and high expression was associated with a longer survival time. Overexpressing LPCAT3 reduced cell proliferation, migration and invasion via enhancing ferroptosis and decreasing the survival signaling; these behaviors were enhanced in LPCAT3-downknocked cells, where a higher abundance of arachidonic acid was observed followed by up-regulation of the downstream survival signaling. In vivo, up-regulation of LPCAT3 decreased tumor growth, but down-regulation enhanced tumor growth and metastasis.
Conclusions: LPCAT3 modulated metabolism of arachidonic acid, thereby regulating ferroptosis and the survival signaling to determine cancer growth and metastasis.

Introduction

Ovarian cancer is the leading cause of cancer-related death in women, with 57,090 newly diagnosed and 39,306 death cases in China in 2022 [1,2]. The 5-year survival rate has been approximately 30% over the past two decades despite the introduction of certain novel agents such as poly-ADP-ribose polymerase inhibitors, attributing to high recurrence and metastasis [3,4]. Therefore, underlying mechanisms need to be thoroughly explored.

Ferroptosis, as a form of programmed cell death, is initiated by lipid peroxidation (LPO) [5]. The central step of implementing ferroptosis is iron-dependent peroxidation of phospholipids [6]. Accumulation of phospholipid hydroperoxides (PLOOH) in cell membranes is a sign of ferroptosis [7]. Glutathion peroxidase 4 (GPX4) eliminates PLOOH. Inactivation of GPX4 causes accumulation of PLOOH, leading to ferroptosis [8]. Ferroptosis is considered a protective mechanism, since inhibiting ferroptosis promotes cancer progression [9,10]. Multiple genes have been identified to regulate ferroptosis [11].

Lysophosphatidylcholine acyltransferase 3 (LPCAT3) is a critical regulator of polyunsaturated fatty acid containing phospholipid (PUFA-PL) [12,13]. LPCAT3 incorporates arachidonic acid (AA; 20:4) into PL to form PUFA-PL species such as phosphatidylethanolamine containing AA (PE-AA) [14]. The presence of oxidized PE-AA in cell membranes can trigger ferroptosis [15,16]. Cytosolic phospholipase A2 (cPLA2) releases AA from phospholipids in the nuclear and plasma membranes [17]. AA enhances the intestinal regeneration via activating WNT signaling, and induces migration of endothelial cells in prostate cancer by activating Rho signaling [18,19]. AA and its metabolites can modulate multiple signaling pathways such as mTORC1/VEGR, NF-κB, MAPK/JNK/p38, PI3K/Akt and epigenetic modifications, thereby inhibiting apoptosis and promoting survival, proliferation, invasion and metastasis of epithelial cancer cells [20,21]. These data indicate that the localization of AA and its metabolites determines the fate of cell survival. However, the role of LPCAT3 in ovarian cancer has been limitedly understood.

* Corresponding author.
E-mail addresses: limin@cqmu.edu.cn (M. Li), yutinghe@hotmail.com (T. Yu).
[1] These authors contributed equally to this work.

https://doi.org/10.1016/j.tranon.2024.102256
Received 14 May 2024; Received in revised form 30 November 2024; Accepted 23 December 2024

The aim of this study was to explore the role of LPCAT3 in serious ovarian cancer. The LPCAT3 expression in cancer tissues was assayed, and then the biological functions were determined in vitro and in vivo. Preliminary data indicated that LPCAT3 modulated proliferation and metastasis of ovarian cancer, and that overexpressing LPCAT3 induced ferroptosis.

Materials and methods

Bioinformatics analyses of gene expression

STAR-counts data and associated clinical information for ovarian tumors were downloaded from the TCGA database (https://portal.gdc.cancer.gov), then extracted in TPM format and performed normalization using the $\log_2$(TPM+1) transformation. After retaining samples that included both RNAseq data and clinical information, 376 samples were selected for further analysis ultimately. Ferroptosis-related genes were based on the data of Liu et al. [22]. Microarray data (GSE63885 and GSE26193) were downloaded from the Gene Expression Omnibus (GEO) (http://www.ncbi.nih.gov/geo). The relationship between LPCAT3 expression and survival in patients with serous ovarian cancer was analyzed using the Kaplan-Meier plotter (http://kmplot.com/analysis/index.php?p=service&cancer=ovar). The matrix of expression of LPCAT3 mRNA in ovarian cancer cell lines was acquired from the CCLE dataset (https://portals.broadinstitute.org/ccle).

Patients and tissue samples

A total of 158 cases of ovarian cancer (01/2013–03/2021) were collected from the Second Affiliated Hospital, Chongqing Medical University (Chongqing, China). Cancer tissues were sampled, and the survival time was noted. The use of human tissues was authorized by the Institutional Review Board.

Immunohistochemistry (IHC)

LPCAT3 protein in cancer tissues was detected with an IHC assay, using a streptavidin-biotin–peroxidase complex kit (Boster Bio., Wuhan, China). Images were analyzed using the software Image J (NIH, Bethesda, MD). The expression level of LPCAT3 was determined using the IHC profiler: negative (1+), low positive (2+), positive (3+) and high positive (4+) [23]. To evaluate the relationship between the expression level and overall survival (OS), high positive and positive were classified as high expression, while low positive and negative were as low expression.

Cells

Human ovarian cancer cell lines SKOV3 (RRID:CVCL_0C84) (identified by STR; Cell Bank, Type Culture Collect, Chinese Academy of Sciences, Shanghai, China) and OVCAR3 (RRID:CVCL_0465) (identified by STR; Xiamen Yimo Biotechnology Co., Xiamen, China) were cultured in RPMI 1640 medium (Gibco, Beijing, China) supplemented with 10% fetal bovine serum (Biol. Ind., Kibbutz, Beit Haemek, Israel), at 5% CO_2 and 37 °C. All experiments were performed with mycoplasma-free cells.

Cell transfection

LPCAT3-overexpressed (LPCAT3 OE) and control (LPCAT3 OE Ctrl), and LPCAT3-downknocked (shLPCAT3) and control (shNC) lentivirus vectors, were obtained from Gene Tech (Shanghai, China). Overexpression was conducted in SKOV3 and OVCAR3 cells, while knockdown was performed in OVCAR3 cells. Vectors were transfected into cells using HiTransG P reagent (Gene Tech). 2.5 μg/mL puromycin (Beyotime, Shanghai, China) was added to the medium to remove uninfected cells. Reverse transcription–quantitative polymerase chain reaction (RT–qPCR) and western blot were used to verify transfection (Fig S1).

Colony formation assay

The colony formation assay was performed on a 6-well plate. 200 cells were seeded and the number of clones was counted after 14 days.

Cell proliferation assay with EdU staining

An EdU kit (Beyotime) was used to assay cell proliferation. Cells (5×10^3) were seeded on a 96-well plate, and proliferation was assessed after 24 h

Wound healing assay

A wound healing assay was used to determine the impact of LPCAT3 on cell migration. Cells were seeded into a 6-well plate. A linear scratch wound was created using a 10-μL pipette tip when the cell confluence reached about 95%. Cells were rinsed with phosphate buffer saline to eliminate those floating cells, and then cultured 24 h The scratch area was measured at the start (0 h) and end (24 h) of the experiment. The rate of cell migration was calculated: [(gap at 0 h – gap at 24 h) / gap at 0 h] × 100%.

Invasion assay

A 8.0-μm pore size transwell insert (Corning Costar, Corning, NY) was used. The upper chamber was coated with matrigel (50 μL), and incubated at 37 °C overnight. Cells (5.0×10^4) were seeded into the upper chamber, while the lower chamber contained 600 μL complete medium. After 24 h, cells in the lower chamber were fixed with 4% paraformaldehyde, stained with methylene blue, and then counted.

Lipidomic analyses using liquid chromatography tandem mass spectrometry (LC–MS)

LPCAT3-overexpressed and -downknocked OVCAR3 cells (1.0×10^7 cells) were stored at −80 °C until LC–MS analyses. Samples were transferred to a glass vial for lipid extraction using dichloromethane/methanol (3:1), and cells were ultrasonically ruptured in an ice bath. Extracts were kept at −20 °C overnight, centrifuged (4 °C, 25,000 g for 15 min), and then lyophilized. Samples were reconstituted in 120 μL of reconstitution solution (isopropanol : acetonitrile : water = 2 : 1 : 1) before LC–MS.

Lipid metabolites were detected using an ACQUITY UPLC I-class plus (Waters, Framingham, MA) tandem Q-Exactive high resolution mass spectrometer (Thermo Fisher Scientific, Waltham, MA) system. A CSH C18 column (1.7 μm, 2.1 × 100 mm; Waters) was used. Mobile phase A was 60% acetonitrile in 10 mM ammonium formate, with 0.1% formic acid; mobile phase B was 90% isopropanol and 10% acetonitrile in 10 mM ammonium formate, with 0.1% formic acid. The gradient was: 40–43 % B at 0–2 min, 43–50 % B at 2–2.1 min, 50–54 % B at 2.1–7 min, 54–70 % B at 7–7.1 min, 70–99 % B at 7.1–13 min, 99–40 % B at 13–13.1 min, and 40% B at 13.1–15 min.

The conditions for MS were: the spray voltage was 3.8 kV for positive mode and 3.2 kV for negative mode, the capillary temperature was 320 °C, the rate of sheath gas flow was 40 arb units, the rate of auxiliary gas flow was 10 arb units, the mass range (m/z) was 200–2000, the full MS resolution was 70,000, the MS/MS resolution was 17,500, the top N value was 3, and the stepped normalized collision energy was sequentially set to 15, 30 and 45 eV The duty cycle for the analysis was 1.2 s.

Metabolites data were processed with the software LipidSearch v.4.1 (Thermo Fisher Scientific), and statistical analyses were performed using the software metaX (http://metax.genomics.cn) [24]. Kyoto Encyclopedia of Genes and Genomes (KEGG) pathway analysis was used

to identify pathways; $p < 0.05$ was set as significance, and the top 10 metabolic pathways with the most metabolites were drawn.

Detection of intracellular iron

Intracellular Fe^{2+} was determined with a colorimetric assay (Elabscience, Wuhan, China) after 24 h, and was normalized to the protein concentration.

Intracellular reactive oxygen species (ROS)

Intracellular ROS was detected with a dihydroethidium assay (BestBio, Shanghai, China) after 24 h

Malondialdehyde measurement (MDA)

Intracellular MDA was measured (Beyotime), and was normalized to the protein concentration.

Cell survival after inhibiting apoptosis or ferroptosis

The apoptosis inhibitor Z-VAD-fmk (Z-VAD; 10 μM; Beyotime), or ferroptosis inhibitor ferrostatin-1 (Fer; 2 μM; MedChemExpress, Shanghai, China) was added to medium. Cell viability was determined after 24 h using a CCK8 assay (Glpbio, Montclair, CA).

Determination of prostaglandin E2 (PGE2)

Intracellular PGE2 was detected using an enzyme-linked immunosorbent assay (Meike, Yancheng, China).

RT–qPCR

Expression levels of LPCAT3, and secreted, cytosolic and calcium-independent phospholipase A2 (sPLA2, cPLA2 and iPLA2) were quantified using RT-qPCR. Total RNA was extracted (TRIzol reagent; Glpbio), cDNA was synthesized (PrimeScript RT Master Mix; Takara Bio., Shiga, Japan), and then qPCR was performed (TB Green Premix Ex Taq II; Takara). GAPDH was the reference. The primer sequences were listed in Table S3.

Western blotting

LPCAT3, GPX4, epidermal growth factor receptor (EGFR), mechanistic target of rapamycin (mTOR), phosphorylated mTOR (p-mTOR), serine/threonine kinase (Akt) and phosphorylated Akt (p-Akt) proteins were detected with western blot, using rabbit antibodies (Cell Signal. Technol., Danvers, MA; Table S4). Bands were analyzed with the software Image Lab (Bio-Rad Lab., Hercules, CA).

Subcutaneous tumors in nude mice

All animal procedures received the ethical approval from the Institutional Review Board (IACUC—CQMU-2023–0013). Female BALB/c nude mice, aged 4–6 weeks and weighed 15–16 g, were randomly divided into 4 groups with 5 mice per group: LPCAT3 OE Ctrl, LPCAT3 OE, shNC and shLPCAT3. Lentivirus-transfected OVCAR3 cells (2.0×10^6) were subcutaneously injected into the right axilla. Body mass and tumor volume (length × width^2/2) were followed, and mice were euthanized after 6 weeks. LPCAT3 and Ki67 in tumor tissues were detected using IHC.

Peritoneal metastasis in nude mice

shNC- or shLPCAT3-transfected OVCAR3 cells (1×10^7) were intraperitoneally injected into female BALB/c nude mice (3 mice per group). Live imaging was acquired when the tumor was palpable. Mice were euthanized after 7 weeks, and intraperitoneal tumor and metastasis were observed.

Statistical analyses

The statistics software GraphPad Prism (GraphPad Software, San Diego, CA) and SPSS (SPSS Inc., Chicago, IL) were used. Student's t-test and analysis of variance were used for normal-distributed quantitative data, while the rank sum test was adopted for nonnormal data. Qualitative data were analyzed using the chi-square test. Survival curves were analyzed with the Kaplan-Meier method; p value and hazard ratio (HR) with 95% confidence intervals (CI) were generated using the log-rank test and univariate Cox proportional hazards model. The critical value was set $p < 0.05$.

Results

High LPCAT3 level in serous cancer tissues indicated a longer survival time

Bioinformatic data indicated that the mRNA level of LPCAT3 was positively correlated with the expression level of ferroptosis-related genes and prognosis (Fig. 1A). Analyses on the GSE63885 and GSE26193 datasets indicated that the expression level of LPCAT3 in serous ovarian cancer was lower than that in other types of epithelial ovarian cancer; KM analysis showed that serous ovarian cancer patients with a low expression level of LPCAT3 gene in cancer tissues had a shorter OS in comparison with those with a high expression level (p = 0.0470, 0.0410) (Figure S1).

LPCAT3 protein in ovarian cancer tissues was assayed. The majority of patients were with stage III and IV diseases (127/158), with the predominant histological type being serous (114/158). The expression level of LPCAT3 correlated with pathological type ($p < 0.0001$) and FIGO stage ($p < 0.0001$) (Table S1, S2). The percentage of low LPCAT3 expression was 80.7% in serous cancer, and was 25.0% in other epithelial cancers ($p < 0.0001$) (Fig. 1B, C). In serous cancer, patients with low LPCAT3 expression in cancer tissues had a shorter OS compared to those with high expression (33 [95% CI, 30.26–37.56] vs. 47 [95% CI, 40.56–54.40] months; $p = 0.0100$) (Fig. 1D). These data indicated that the LPCAT3 level in serous cancer tissues impacted on the survival.

Overexpressing LPCAT3 decreased cell proliferation, migration and invasion

The basal expression level of LPCAT3 was low in SKOV3 cells and was moderate in OVCAR3 cells. Thus, overexpression was induced in both SKOV3 and OVCAR3 cells, and knockdown was induced in OVCAR3 cells, which was verified by RT−qPCR and western blot (Figure S2, S3). Overexpressing LPCAT3 reduced clone formation, proliferation, migration and invasion in SKOV3 (p = 0.0001–0.0074) and OVCAR3 cells (p = <0.0001 to 0.0154) (Fig. 2). These data showed that overexpressing LPCAT3 decreased proliferation and invasion of ovarian cancer cells.

LPCAT3 altered the lipid profile

Given the role of LPCAT3 in lipid metabolism, lipid metabolites were determined in LPCAT3-overexpressed and -downknocked OVCAR3 cells. Of those identified 959 metabolites, the top two abundant metabolites were phosphatidylcholine (PC) and PE; the content of total lipids in downknocked cells was lower than that in overexpressed cells (PC: LPCAT3 OE Ctrl vs. LPCAT3 OE, $p = 0.0077$; LPCAT3 OE vs. shLPCAT3, $p = 0.0060$. PE: LPCAT3 OE Ctrl vs. LPCAT3 OE, $p = 0.0007$, LPCAT3 OE vs. shLPCAT3, $p = 0.0030$. Total: LPCAT3 OE Ctrl vs. LPCAT3 OE, $p = 0.0040$, LPCAT3 OE vs. shLPCAT3, $p = 0.0010$)

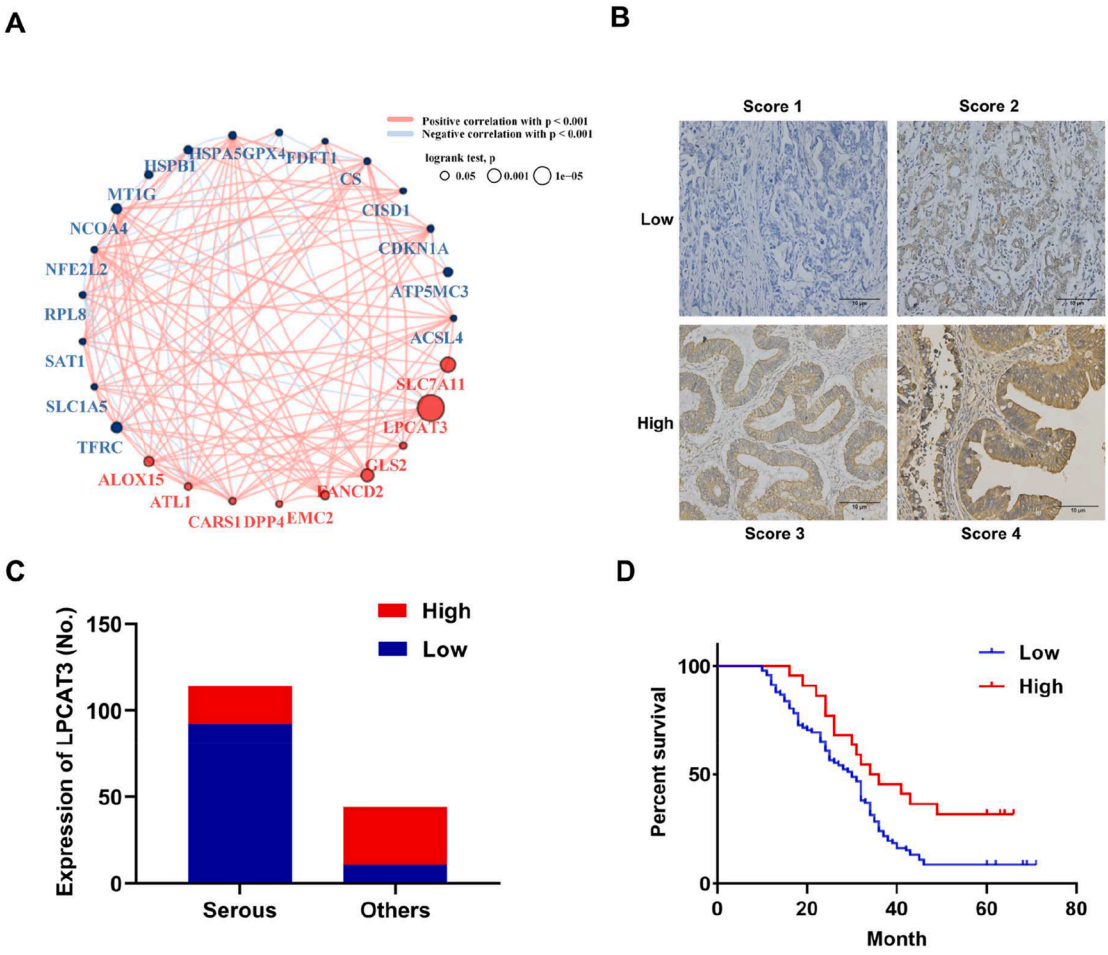

Fig. 1. Expression of LPCAT3 in serous ovarian cancer. (**A**) Expression pattern of ferroptosis-related genes in ovarian cancer: a red dot indicated a positive correlation, while a blue dot showed a negative correlation (a larger size represented a lower p value for prognosis); data indicated that LPCAT3 was correlated with ferroptosis. (**B**) Representative images of LPCAT3 staining in ovarian cancer tissues: the scale bar was 10 μm. (**C**) Expression level of LPCAT3: the percentage of low expression in serous cancer was higher than that in other cancer type. (**D**) Correlation between the LPCAT3 expression level and survival in patients with serous cancer: patients with high expression in cancer tissues (n = 22) had a longer survival time compared with those with low expression (n = 92).

(Fig. 3A–D). There were 635 differentially expressed metabolites (fold-change ≥1.2 or ≤0.83, p < 0.05) between overexpressed and down-knocked cells, where 332 items were up-regulated and 303 items were down-regulated (Fig. 3E). KEGG analyses showed that AA metabolism was the first-ranked pathway (Fig. 3F). These data indicated that LPCAT3 can modulate the profile of lipid metabolites.

Overexpressing LPCAT3 induced ferroptosis and down-regulated the survival signaling

PE-AA was analyzed considering its role in ferroptosis [25]. Overexpression of LPCAT3 increased the abundances of PE-AA (p < 0.0100) (Fig. 4A). Levels of Fe^{2+}, ROS and MDA were increased in overexpressed cells (SKOV3: p = <0.0001 to 0.0249; OVCAR3: p = <0.0001 to 0.0021), but that of GPX4 was decreased (SKOV3: p = 0.0249; OVCAR3: p = 0.0036) (Fig. 4B–F). The decrease in cell-survival due to LPCAT3 overexpression was alleviated by Fer, but this effect was not detected after using Z-VAD (SKOV3: p = 0.0003; OVCAR3: p < 0.0001) (Fig. 4G).

cPLA2 released AA from cell membranes; cPLA2-mediated signals were involved in communication between cancer and endothelial cells via the AA-cascade signaling pathway, thereby regulating multiple aspects of cancer progression including survival, proliferation, apoptosis and metastasis [26,27]. PGE2 derived from AA, and promoted cancer proliferation and metastasis [28]. The level of cPLA2 was decreased in LPCAT3-overexpressed cells (SKOV3: p = 0.0187; OVCAR3: p = 0.0036), and those of AA and PGE2 were decreased (AA: p < 0.0001 for each. PGE2: LPCAT3 OE Ctrl vs. LPCAT3 OE, p < 0.0001 for each; shNC vs. shLPCAT3, p = 0.0003) (Fig. 5A–D). Western blot indicated that levels of p-Akt, p-mOTR and EFGR were decreased after overexpressing LPCAT3 (SKOV3: p = <0.0001 to 0.0054; OVCAR3: p = <0.0001 to 0.0002) (Fig. 5E–G). These data indicated that overexpressing LPCAT3 increased the amount of PE-AA and down-regulated the survival signaling, thereby inducing ferroptosis and reducing cell proliferation.

Downknocking LPCAT3 promoted cell proliferation and invasion via activating AKT/mTOR signaling

Downknocking LPCAT3 promoted clone formation, proliferation, migration and invasion in OVCAR3 cells (p = 0.0003–0.0057) (Fig. 2). The abundance of PE-AA was decreased (p < 0.0001 for each) (Fig. 4A). However, no alterations were detected in levels of Fe^{2+}, MDA and GPX4 (p = 0.0532–0.1005) (Figure 4B–*F*).

The level of cPLA2 was increased in LPCAT3-downregulated cells (p = 0.0017), and those of AA and PGE2 were increased (p < 0.0001 for each) (Fig. 5A–D). AA-induced cell migration and invasion was mediated by Akt/PI3K and EGFR pathways [29]. Levels of p-mTOR, p-Akt and EGFR proteins were increased in LPCAT3-downknocked cells (p = <0.0001 to 0.0048) (Fig. 5E, F). These data indicated that down-regulating LPCAT3 upregulated the metabolism of AA to increase PGE2, thereby activating the survival signaling to promote cell proliferation,

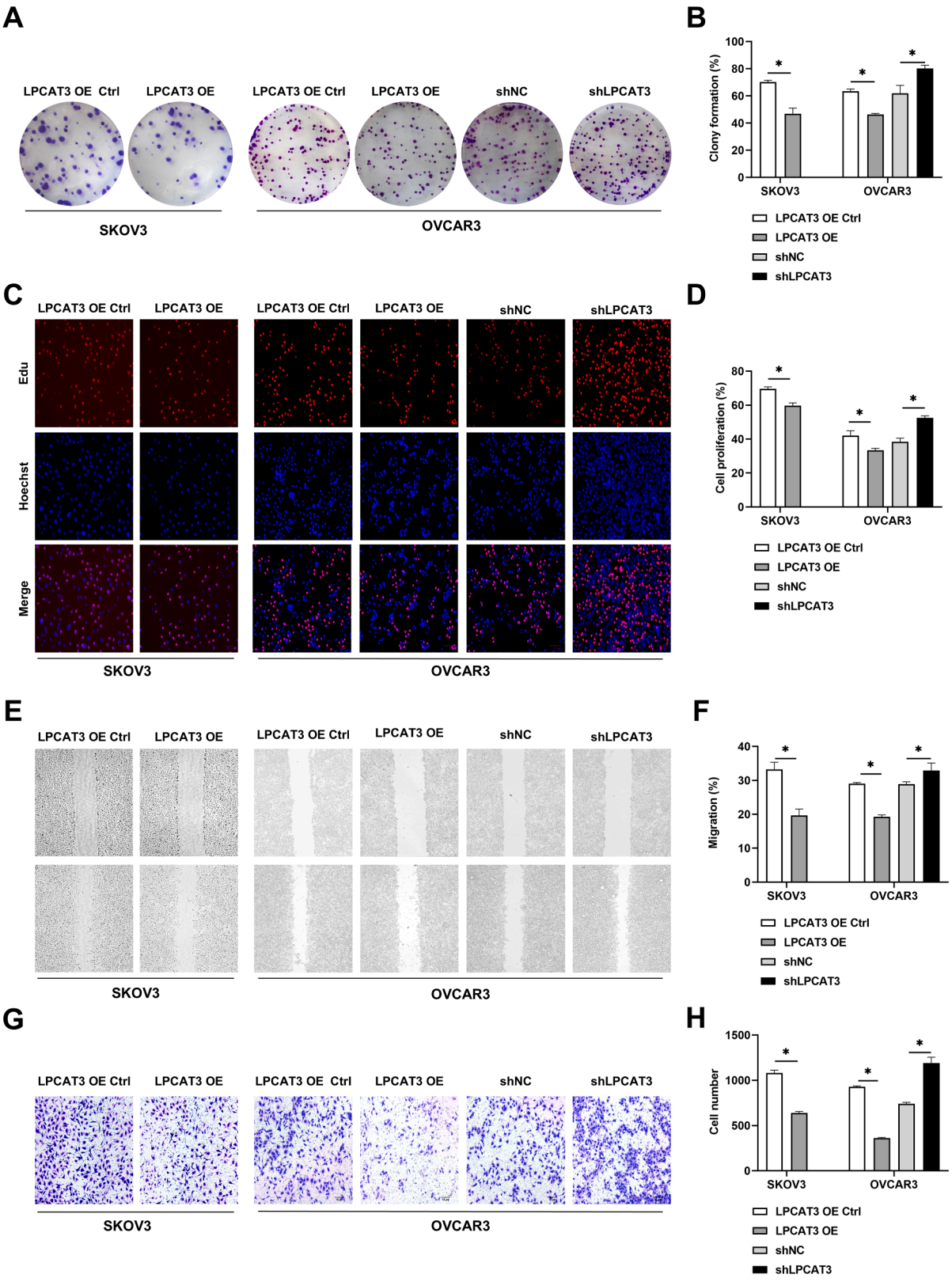

Fig. 2. LPCAT3 regulated cellular proliferation, migration and invasion. (**A, B**) Clone formation: overexpression decreased clone formation but knockdown increased clone formation. (**C, D**) Cell proliferation, (**E, F**) migration, and (**G, H**) invasion: these behaviors were increased in LPCAT3-downknocked cells, but were decreased in -overexpressed cells. Data were mean ± standard deviation for 3 independent trials. *: $p < 0.05$.

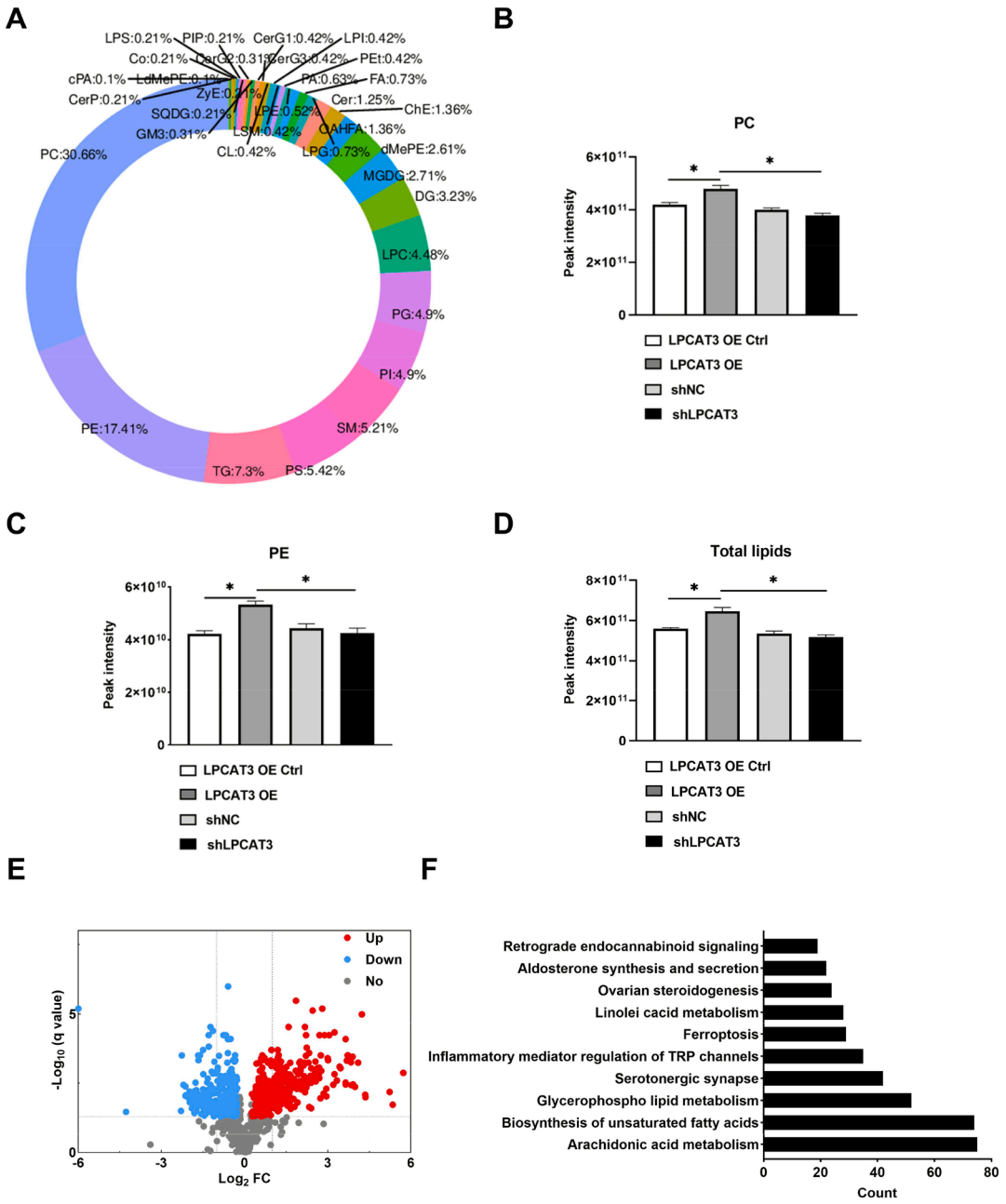

Fig. 3. Lipid profiles in LPCAT3-overexpressed and -downknocked OVCAR3 cells. (**A**) Classification of lipid metabolites. (**B, C**) Intensities of PC and PE: both were increased in overexpressed cells. (**D**) Total lipids: the content was increased in overexpressed cells. (**E**) Volcano plot of differential metabolites. (**F**) Metabolic pathway enrichment: AA metabolism ranked the first. *: $p < 0.05$.

migration and invasion.

LPCAT3 impacted cancer growth and metastasis in vivo

In the subcutaneous tumors, the tumor volume was reduced in group LPCAT3 OE in comparison with group LPCAT3 OE Ctrl, and the volume in group shLPCAT3 was larger than that in group shNC ($p < 0.0010$ for each). Tumor mass displayed the same trend ($p = 0.0085$–0.0290) (Fig. 6A–C). LPCAT3 and Ki67 in tumor tissues were assayed. The LPCAT3 level was increased in group LPCAT3 OE, but the Ki67 level was decreased ($p = 0.0115$, 0.0010); opposite effects were detected after downknocking LPCAT3, i.e., a lower LPCAT3 with a higher Ki67 levels ($p = 0.0096$, <0.0001) (Fig. 6D–G).

In the peritoneal metastasis model, more metastatic foci were observed in group shLPCAT3 compared to group shNC ($p = 0.0158$) (Fig. 6H–J). These data indicated that downregulating LPCAT3 promoted cancer growth and metastasis, but that overexpressing LPCAT3 reduced cancer growth.

Discussion

Ferroptosis can cause cell death and enhance chemotherapy, thereby being a strategy to combat cancers including chemoresistant ones [30–32]. Here demonstrated that serious ovarian cancer patients with high LPCAT3 expression in cancer tissues had a longer survival time, and that up-regulating LPCAT3 induced ferroptosis to decrease cell proliferation, migration and invasion. Therefore, LPCAT3 played a part in cancer progression.

Integration of PUFA into membrane PL was necessary for LPO to induce ferroptosis. PUFA-PL reacted with Fe^{2+}, increasing the amount of

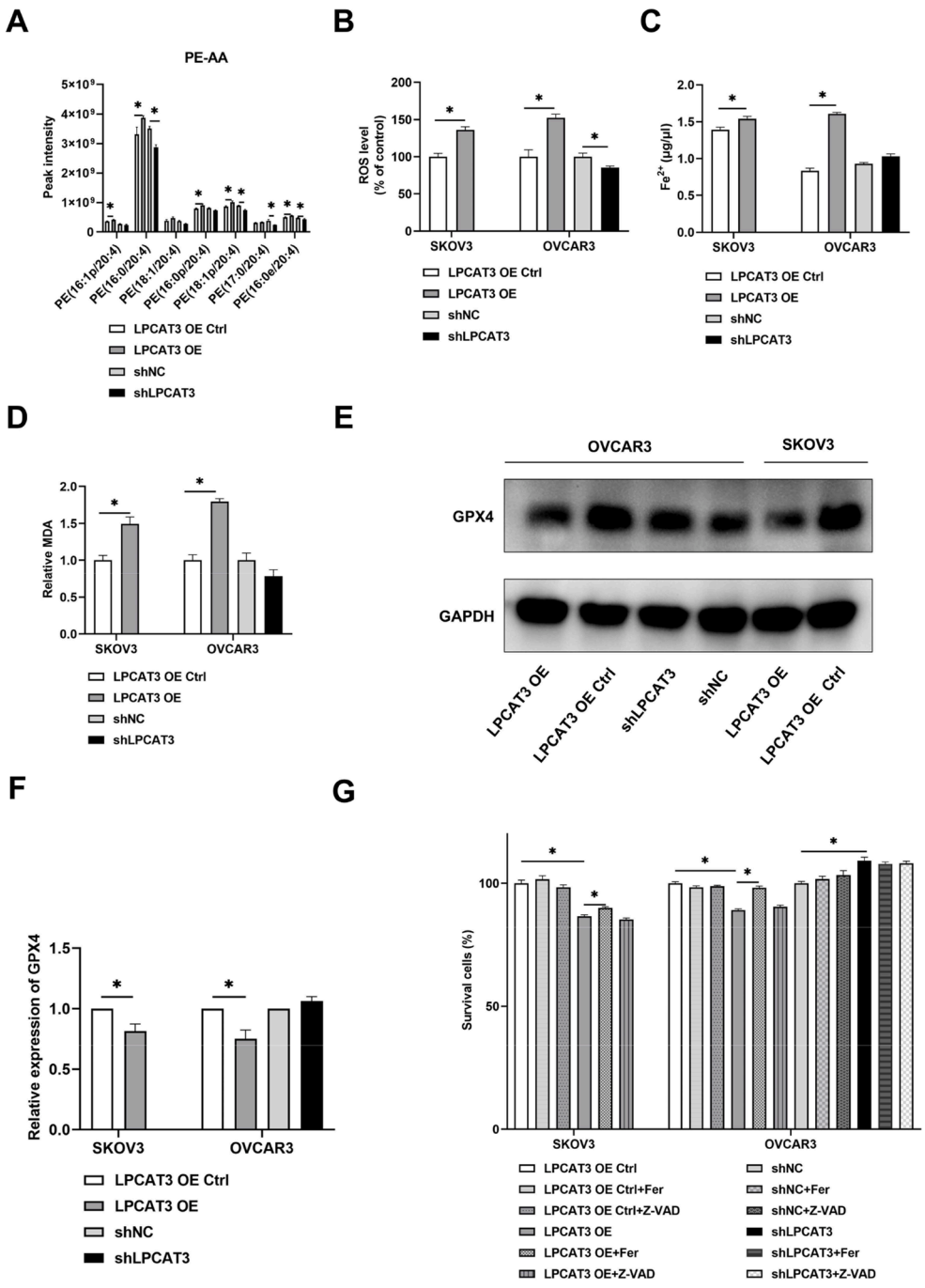

Fig. 4. LPCAT3 induced ferroptosis via AA pathway. (**A**) Intensities of PE−AA: the intensity was increased in overexpressed cells. (**B**−**D**) Intracellular levels of ROS, Fe^{2+} and MDA: higher levels were detected in overexpressed cells. (**E, F**) GPX4: the expression level was reduced in overexpressed cells. (**G**) Cell-survival percentages after adding Fer or Z-VAD: Fer increased the survival percentage in LPCAT3-overexpressed cells. Data were mean ± standard deviation for 3 independent trials. *: $p < 0.05$.

PUFA-PL-OOH to enhance LPO [33]. Fe^{2+} and H_2O_2 generated hydroxyl radicals (·OH) and superoxide radicals (·O2) i.e., the Fenton reaction, and those ROS caused LPO [34]. Here LPCAT3 altered the lipidomic profile in ovarian cancer cells. LPCAT3 involved in acylation of AA to membrane PL [35,36]. Lipidomics indicated that overexpressing LPCAT3 increased the amount of PE-AA, being consistent with data of Conrad et al. [37]. PE-AA was oxidized under Fe^{2+}, thereby triggering ferroptosis [38]. GPX4 can scavenge lipid ROS; thus a decrease favored ferroptosis [39]. MDA was the product of PUFA peroxidation. Increases in levels of Fe^{2+}, ROS and MDA, and a decrease in GPX4 demonstrated ferroptosis in LPCAT3-overexpressed cells. Occurrence of ferroprosis was confirmed by Fer increasing the cell-survival percentage. cPLA2 released AA from membrane PL [40,41]. Overexpressing LPCAT3 down-regulated cPLA2, thereby reducing amounts of free AA and PUFA. This was consistent with data of Koundouros et al. [26]. These effects eventually increased the accumulation of oxidized PE-AA in cell membranes to initiate ferroptosis, and ferroptosis was amplified by higher levels of Fe^{2+} and ROS and a low level of GPX4. Levels of EGFR, p-Akt and p-mTOR were decreased in overexpressed cells. EGFR/AKT/mTOR was the survival signaling [42]. AA was the precursor for synthesizing PGE2, the reduction in AA decreased the PGE2 level, and EGFR/AKT/mTOR was the downstream signal pathway of PGE2. Thus,

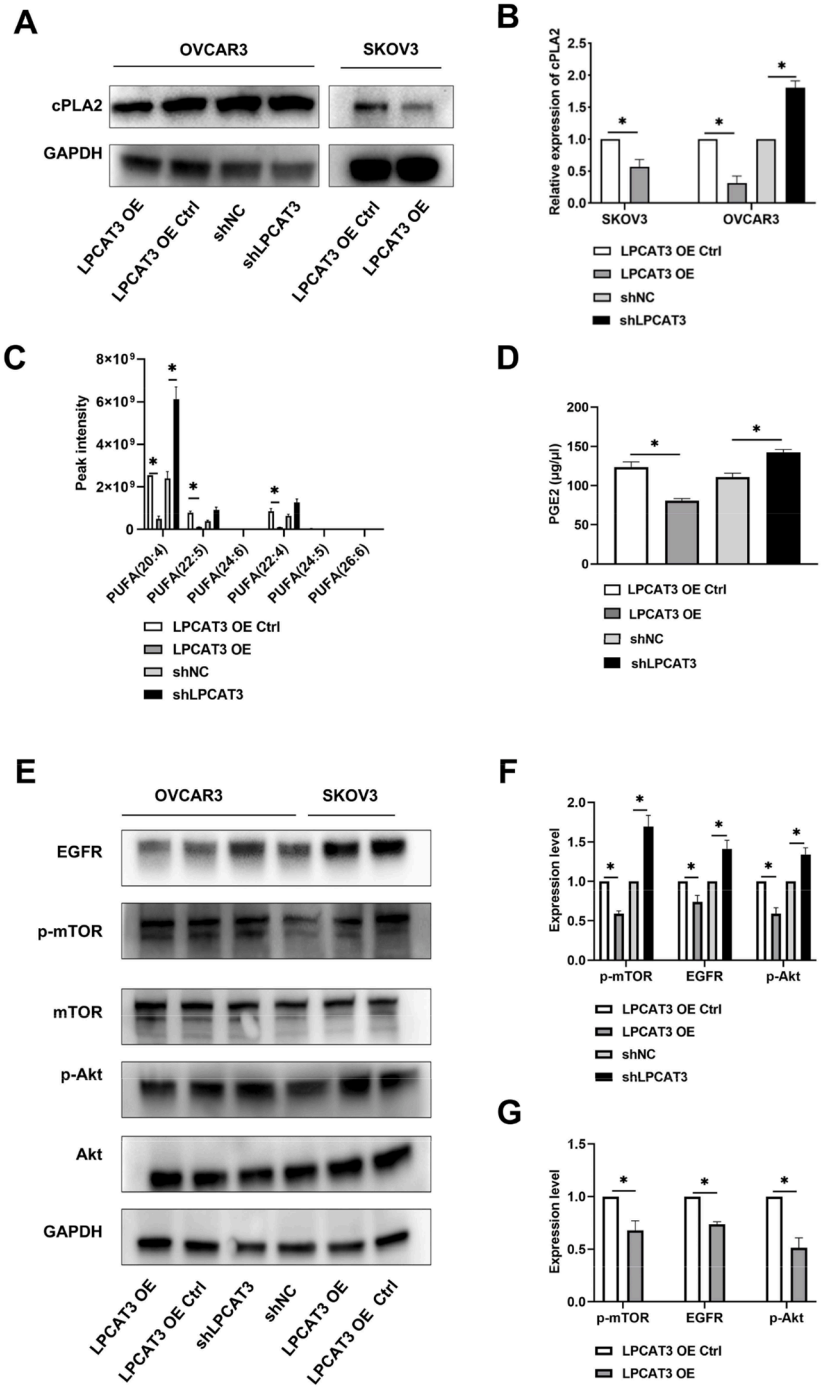

Fig. 5. Downknocking LPCAT3 promoted proliferation and metastasis of serous ovarian cancer via activating the AKT/mTOR signaling pathway. (**A, B**) cPLA2: the expression level was decreased in LPCAT3-overexpressed cells, but was increased in -downknocked cells. (**C**) PUFA: intensities of certain items were decreased in overexpressed cells, but were increased in downknocked cells. (**D**) PGE2 level: a lower level was noted in overexpressed cells, but a higher level was detected in downknocked cells. (**E−G**) Expression of EGFR, Akt, and mTOR: downknocking LPCAT3 activated EGFR/Akt/mTOR pathway, but overexpressing LPCAT3 led to opposite effects. Data were mean ± standard deviation for 3 independent trials. *: $p < 0.05$.

overexpressing LPCAT3 enhanced ferroptosis and decreased survival signaling, thereby suppressing cell proliferation and invasion.

The level of PE-AA was decreased in LPCAT3-downknockded cells. In vitro cell proliferation, migration and invasion were promoted. However, features of Fe^{2+}, ROS, MDA and GPX4 did not support a reduction on ferroptosis. Therefore, enhancement of these invasive behaviors was due to other mechanisms. The cPLA2 level was decreased in LPCAT3-downknockded cells, which increased the level of free AA. More AA increased the level of PGE2. PGE2 can activate the survival signal pathway EGFR/Akt/mTOR to favor cell proliferation and invasion [28, 43]. These were consistent with the present data that levels of AA, PGE2, EGFR, p-Akt and p-mTOR were up-regulated in downknocked cells.

In vivo data confirmed the role of LPCAT3 in ovarian cancer. Overexpressing LPCAT3 reduced the tumor volume/mass, but suppressing LPCAT3 increased the tumor burden. The Ki67 level in tumor tissues that reflected cell proliferation was inversely correlated with that of LPCAT3. In the peritoneal metastasis model, downknocking LPCAT3 enhanced metastasis, being consistent with enhanced cell migration and

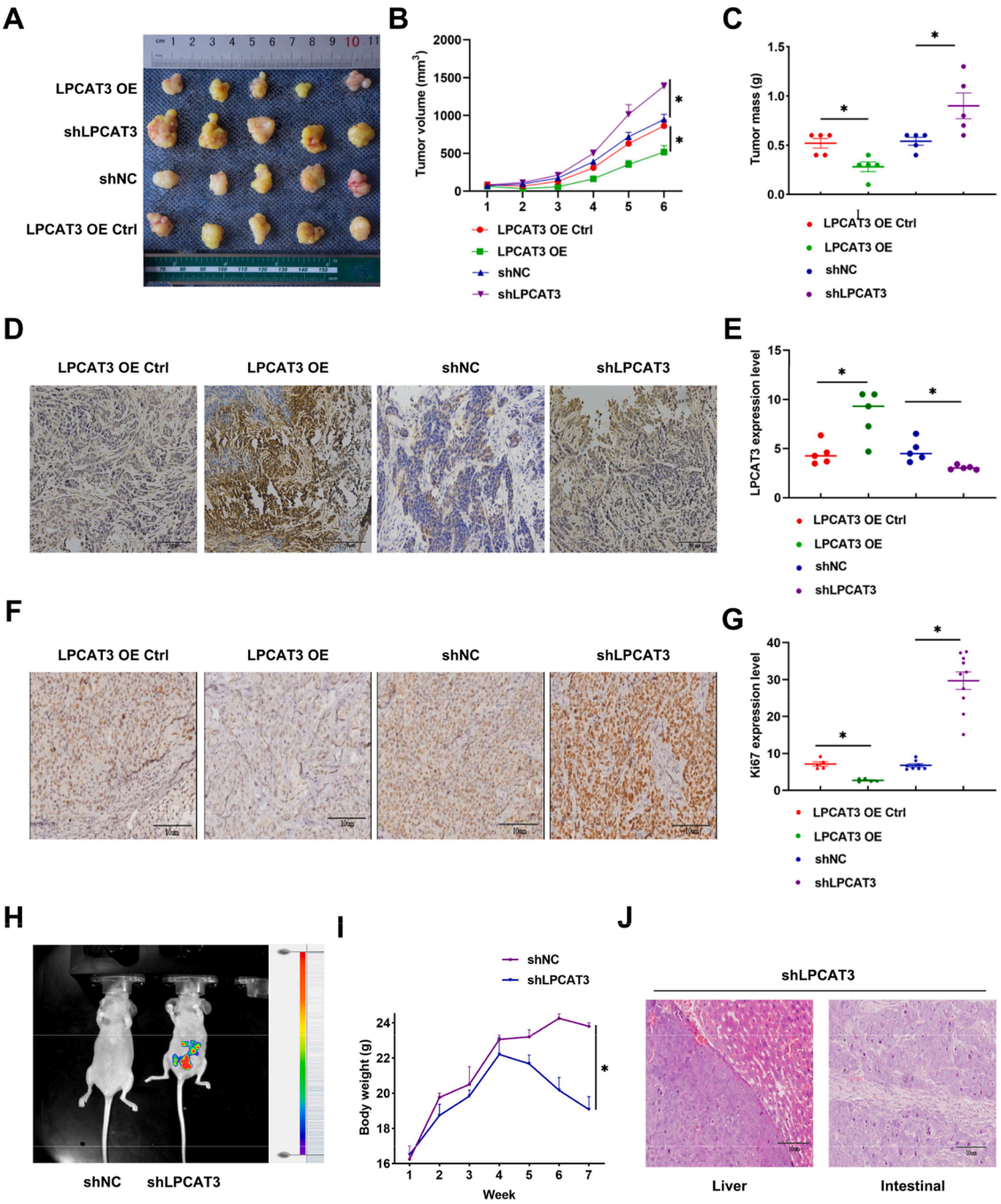

Fig. 6. LPCAT3 regulated cancer proliferation and metastasis in vivo. (**A–C**) Subcutaneous tumors in mice: tumor growth was reduced in group LPCAT3 OE, but was enhanced in group shLPCAT3. (**D–G**) Expression of LPCAT3 and Ki67 in tumor tissues: the level of Ki67 was inversely correlated with that of LPCAT3. (**H–J**) Intraperitoneal metastasis: more foci were noted in group shLPCAT3; pathological examinations confirmed liver and intestinal metastasis; a decrease on body mass was observed in group shLPCAT3. Data were mean ± standard deviation. *: $p < 0.05$.

invasion in vitro; a decrease on body mass was observed in group shLPCAT3, which was mainly due to more rapid growth and spread of tumors.

Conclusions

LPCAT3 impacted on the behaviors of serous ovarian cancer; patients with high expression in cancer tissues had a longer survival time. LPCAT3 modulated AA metabolism. Overexpression favored the formation of PE-AA in cell membrane to induce ferroptosis and decreased EGFR/Akt/mTOR signaling, thereby suppressing cell proliferation, migration and invasion. Downkncoking LPCAT3 increased the PGE2 level, activated EGFR/Akt/mTOR signaling, and eventually promoted cell proliferation, migration and invasion. Therefore, LPCAT3 was a target for treatment of serious ovarian cancer.

Ethics approval and consent to participate

For patients: this research was approved by the Second Affiliated Hospital, Chongqing Medical University (2023–53). For animals: animal experiments were approved by Chongqing Medical University (2023–0013).

Consent for publication

All authors have reviewed the final version of the manuscript and approve it for publication.

Role of study sponsor or funder

The funding body played no role in the study design, the collection, analysis, or interpretation of data, the writing of the report, or the decision to submit this paper for publication.

Informed consent statement

Informed consents for human participants were not required according to the national legislation and the institutional requirements. The animal study was reviewed and approved by the Ethics Committee of Chongqing Medical University Approval.

Availability of data and material

The original contributions presented in the study are included in the article and supplementary material. Further inquiries can be directed to the corresponding authors.

Funding information

This work was supported by the Postgraduate research and innovation projects of the Chongqing Municipal Education Commission (CYB20152).

CRediT authorship contribution statement

Fang Wen: Writing – original draft, Validation, Methodology, Investigation, Data curation, Conceptualization. **Hongjian Ling:** Writing – original draft, Supervision, Project administration, Funding acquisition, Conceptualization. **Rui Ran:** Resources, Data curation. **Xinya Li:** Writing – review & editing, Investigation, Data curation. **Houmei Wang:** Writing – review & editing, Resources, Funding acquisition. **Qianfen Liu:** Writing – review & editing, Resources. **Min Li:** Writing – review & editing, Resources. **Tinghe Yu:** Writing – review & editing, Supervision, Resources, Project administration, Conceptualization.

Declaration of competing interest

The authors declare that they have no known competing financial interests or personal relationships that could have appeared to influence the work reported in this paper.

Supplementary materials

Supplementary material associated with this article can be found, in the online version, at doi:10.1016/j.tranon.2024.102256.

References

[1] C. Xia, X. Dong, H. Li, M. Cao, D. Sun, S. He, et al., Cancer statistics in China and United States, 2022: profiles, trends, and determinants, Chin. Med. J. 135 (5) (2022) 584–590.
[2] R.L. Siegel, K.D. Miller, H.E. Fuchs, A. Jemal, Cancer statistics, 2022, CA Cancer J. Clin. 72 (1) (2022) 7–33.
[3] S. Moufarrij, M. Dandapani, E. Arthofer, S. Gomez, A. Srivastava, M. Lopez-Acevedo, et al., Epigenetic therapy for ovarian cancer: promise and progress, Clin. Epigenetics 11 (1) (2019) 7.
[4] P.M. Webb, S.J. Jordan, Global epidemiology of epithelial ovarian cancer, Nat. Rev. Clin. Oncol. 21 (5) (2024) 389–400.
[5] S.J. Dixon, K.M. Lemberg, M.R. Lamprecht, R. Skouta, E.M. Zaitsev, C.E. Gleason, et al., Ferroptosis: an iron-dependent form of nonapoptotic cell death, Cell 149 (5) (2012) 1060–1072.
[6] X. Jiang, B.R. Stockwell, M. Conrad, Ferroptosis: mechanisms, biology and role in disease, Nat. Rev. Mol. Cell Biol. 22 (4) (2021) 266–282.
[7] L. Zhao, X. Zhou, F. Xie, L. Zhang, H. Yan, J. Huang, et al., Ferroptosis in cancer and cancer immunotherapy, Cancer Commun 42 (2) (2022) 88–116.
[8] D. Liang, Y. Feng, F. Zandkarimi, H. Wang, Z. Zhang, J. Kim, et al., Ferroptosis surveillance independent of GPX4 and differentially regulated by sex hormones, Cell 186 (13) (2023) 2748–2764. .e22.
[9] D. Ruan, J. Wen, F. Fang, Y. Lei, Z. Zhao, Y. Miao, Ferroptosis in epithelial ovarian cancer: a burgeoning target with extraordinary therapeutic potential, Cell Death. Discov. 9 (1) (2023) 434.
[10] D. Li, M. Zhang, H. Chao, Significance of glutathione peroxidase 4 and intracellular iron level in ovarian cancer cells-"utilization" of ferroptosis mechanism, Inflamm. Res. 70 (10–12) (2021) 1177–1189.
[11] X. Tong, R. Tang, M. Xiao, J. Xu, W. Wang, B. Zhang, et al., Targeting cell death pathways for cancer therapy: recent developments in necroptosis, pyroptosis, ferroptosis, and cuproptosis research, J. Hematol. Oncol. 15 (1) (2022) 174.
[12] A. Reed, T.A. Ichu, N. Milosevich, B. Melillo, M.A. Schafroth, Y. Otsuka, et al., LPCAT3 inhibitors remodel the polyunsaturated phospholipid content of human cells and protect from ferroptosis, ACS Chem. Biol. 17 (6) (2022) 1607–1618.
[13] L. Lagrost, D. Masson, The expanding role of lyso-phosphatidylcholine acyltransferase-3 (LPCAT3), a phospholipid remodeling enzyme, in health and disease, Curr. Opin. Lipidol. 33 (3) (2022) 193–198.
[14] X. Rong, B. Wang, M.M. Dunham, P.N. Hedde, J.S. Wong, E. Gratton, et al., Lpcat3-dependent production of arachidonoyl phospholipids is a key determinant of triglyceride secretion, Elife 4 (2015) e06557.
[15] Z. Li, T. Ding, X. Pan, Y. Li, R. Li, P.E. Sanders, et al., Lysophosphatidylcholine acyltransferase 3 knockdown-mediated liver lysophosphatidylcholine accumulation promotes very low density lipoprotein production by enhancing microsomal triglyceride transfer protein expression, J. Biol. Chem. 287 (24) (2012) 20122–20131.
[16] T. Manivarma, A.A. Kapralov, S.N. Samovich, Y.Y. Tyurina, V.A. Tyurin, A. P. VanDemark, et al., Membrane regulation of 15LOX-1/PEBP1 complex prompts the generation of ferroptotic signals, oxygenated PEs, Free Radic, Biol. Med. 208 (2023) 458–467.
[17] P. Pan, G. Qin, B. Wang, H. Yu, J. Chen, J. Liu, et al., HDAC5 loss enhances phospholipid-derived arachidonic acid generation and confers sensitivity to cPLA2 inhibition in pancreatic cancer, Cancer Res 82 (24) (2022) 4542–4554.
[18] Y. Zhang, Y. Liu, J. Sun, W. Zhang, Z. Guo, Q. Ma, Arachidonic acid metabolism in health and disease, MedComm 4 (5) (2023) e363.
[19] Q. Wang, Y. Lin, X. Sheng, J. Xu, X. Hou, Y. Li, et al., Arachidonic acid promotes intestinal regeneration by activating WNT signaling, Stem Cell Reports 15 (2) (2020) 374–388.
[20] B. Wang, L. Wu, J. Chen, L. Dong, C. Chen, Z. Wen, et al., Metabolism pathways of arachidonic acids: mechanisms and potential therapeutic targets, Signal Transduct. Target Ther. 6 (1) (2021) 94.
[21] A. Ruiz-Saenz, C.E. Atreya, C. Wang, B. Pan, C.A. Dreyer, D. Brunen, et al., A reversible SRC-relayed COX2 inflammatory program drives resistance to BRAF and EGFR inhibition in BRAF(V600E) colorectal tumors, Nat. Cancer 4 (2) (2023) 240–256.
[22] Z. Liu, Q. Zhao, Z.X. Zuo, S.Q. Yuan, K. Yu, Q. Zhang, et al., Systematic analysis of the aberrances and functional implications of Ferroptosis in cancer, iScience 23 (7) (2020) 101302.
[23] F. Varghese, A.B. Bukhari, R. Malhotra, A. De, IHC Profiler: an open source plugin for the quantitative evaluation and automated scoring of immunohistochemistry images of human tissue samples, PLoS One 9 (5) (2014) e96801.
[24] B. Wen, Z. Mei, C. Zeng, S. Liu, metaX: a flexible and comprehensive software for processing metabolomics data, BMC Bioinformatics 18 (1) (2017) 183.
[25] S.N. Samovich, K. Mikulska-Ruminska, H.H. Dar, Y.Y. Tyurina, V.A. Tyurin, A. B. Souryavong, et al., Strikingly High Activity of 15-Lipoxygenase Towards Di-Polyunsaturated Arachidonoyl/Adrenoyl-Phosphatidylethanolamines Generates Peroxidation Signals of Ferroptotic Cell Death, Angew. Chem. Int. Edit. 63 (9) (2024) e202314710.
[26] N. Koundouros, E. Karali, A. Tripp, A. Valle, P. Inglese, N. Perry, et al., Metabolic Fingerprinting Links Oncogenic PIK3CA with Enhanced Arachidonic Acid-Derived Eicosanoids, Cell 181 (7) (2020) 1596–1611. .e27.
[27] Z. Peng, Y. Chang, J. Fan, W. Ji, C. Su, Phospholipase A2 superfamily in cancer, Cancer Lett 497 (2021) 165–177.
[28] C. Xu, L. Gu, L. Hu, C. Jiang, Q. Li, L. Sun, et al., FADS1-arachidonic acid axis enhances arachidonic acid metabolism by altering intestinal microecology in colorectal cancer, Nat. Commun. 14 (1) (2023) 2042.
[29] S. Villegas-Comonfort, R. Castillo-Sanchez, N. Serna-Marquez, P. Cortes-Reynosa, E.P. Salazar, Arachidonic acid promotes migration and invasion through a PI3K/Akt-dependent pathway in MDA-MB-231 breast cancer cells, Prostaglandins Leukot. Essent. Fatty Acids 90 (5) (2014) 169–177.
[30] Q. Liu, X. Li, Y. Luo, H. Wang, Y. Zhang, T. Yu, Ultrasonically Enhanced ZD2767P-Carboxypeptidase G2 Deactivates Cisplatin-Resistant Human Lung Cancer Cells, Oxid. Med. Cell Longev. 2022 (2022) 9191233.
[31] T. Hong, G. Lei, X. Chen, H. Li, X. Zhang, N. Wu, et al., PARP inhibition promotes ferroptosis via repressing SLC7A11 and synergizes with ferroptosis inducers in BRCA-proficient ovarian cancer, Redox Biol 42 (2021) 101928.
[32] L. Jiang, N. Kon, T. Li, S.J. Wang, T. Su, H. Hibshoosh, et al., Ferroptosis as a p53-mediated activity during tumour suppression, Nature 520 (7545) (2015) 57–62.
[33] B.R. Stockwell, Ferroptosis turns 10: emerging mechanisms, physiological functions, and therapeutic applications, Cell 185 (14) (2022) 2401–2421.

[34] F. Zhang, F. Li, G.H. Lu, W. Nie, L. Zhang, Y. Lv, et al., Engineering Magnetosomes for Ferroptosis/Immunomodulation Synergism in Cancer, ACS Nano 13 (5) (2019) 5662–5673.
[35] S.J. Dixon, G.E. Winter, L.S. Musavi, E.D. Lee, B. Snijder, M. Rebsamen, et al., Human haploid cell genetics reveals roles for lipid metabolism genes in nonapoptotic cell death, ACS Chem. Biol. 10 (7) (2015) 1604–1609.
[36] V. Kondreddy, R. Banerjee, B. Devi, K. Muralidharan, S. Piramanayagam, Inhibition of the MALT1-LPCAT3 axis protects cartilage degeneration and osteoarthritis, Cell Commun. Signal. 22 (1) (2024) 189.
[37] M. Conrad, D.A. Pratt, The chemical basis of ferroptosis, Nat. Chem. Biol. 15 (12) (2019) 1137–1147.
[38] S. Doll, B. Proneth, Y.Y. Tyurina, E. Panzilius, S. Kobayashi, I. Ingold, et al., ACSL4 dictates ferroptosis sensitivity by shaping cellular lipid composition, Nat. Chem. Biol. 13 (1) (2017) 91–98.
[39] W.S. Yang, B.R. Stockwell, Ferroptosis: death by Lipid Peroxidation, Trends Cell Biol 26 (3) (2016) 165–176.
[40] A. Hedbrant, I. Persson, A. Erlandsson, J. Wijkander, Green, black and rooibos tea inhibit Prostaglandin E2 formation in human monocytes by inhibiting expression of enzymes in the prostaglandin E2 pathway, Molecules 27 (2) (2022) 397.
[41] F.M. Davis, L.C. Tsoi, R. Wasikowski, A. denDekker, A. Joshi, C. Wilke, et al., Epigenetic regulation of the PGE2 pathway modulates macrophage phenotype in normal and pathologic wound repair, JCI Insight 5 (17) (2020) e138443.
[42] M. Huang, D. Xiong, J. Pan, Q. Zhang, S. Sei, R.H. Shoemaker, et al., Targeting glutamine metabolism to enhance immunoprevention of EGFR-driven lung cancer, Adv. Sci. 9 (26) (2022) e2105885.
[43] R.A. Saxton, D.M. Sabatini, mTOR Signaling in growth, metabolism, and disease, Cell 169 (2) (2017) 361–371.